

Supporting Information for

Magmatic Controls on Volcanic Sulfur Emissions at the Iceland Hotspot

E. Ranta^{1,2}, S. A. Halldórsson¹, B. A. Óladóttir³, M. A. Pfeffer³, A. Caracciolo¹, E. Bali¹, G. H. Guðfinnsson¹, M. Kahl⁴, and S. Barsotti³

¹Nordic Volcanological Center, Institute of Earth Sciences, University of Iceland, Iceland.

²Department of Geosciences and Geography, University of Helsinki, Finland.

³Icelandic Meteorological Office, Iceland.

⁴Institut Für Geowissenschaften, Universität Heidelberg, Heidelberg, Germany.

Corresponding author: Eemu Ranta (eemu.ranta@helsinki.fi)

Contents of this file

Text S1. H₂O, CO₂, F and Cl concentrations of Icelandic melt inclusions

Text S2. Effects of crustal magma evolution on H₂O, CO₂, F and Cl

Figures S1–S11

Additional Supporting Information (Files uploaded separately)

Table S1: Iceland Melt Inclusion Catalogue (IMIC)

Table S2: Summary of volatile emission potentials and average MI and MG compositions

Table S3: EPMA data of matrix glasses

Table S4: EPMA data of melt inclusions

Table S5: EPMA data of plagioclase

Table S6: EPMA data of olivine and clinopyroxene

Table S7: EPMA data of glass and mineral standards

Table S8: Melting model parameters

Introduction

This file contains an overview of the non-S volatiles and the Supplementary Figures S1–S5. Supplementary Tables S1–S8 are provided as separate Excel-files.

S1. H₂O, CO₂, F and Cl concentrations of Icelandic melt inclusions

Water: Water contents of Icelandic melt inclusions vary from <0.1 wt.% in trace element-depleted rift basalts to up to 6.5 wt.% in silicic melt inclusions from Hekla. Overall, H₂O concentrations increase with increasing SiO₂ (Fig. 3a) and are lowest in basaltic MIs (0-1.5 wt.‰), moderate in intermediate MIs (0.7-4 wt.%) and highest, but also highly variable in silicic melts (0.1 to 6.5 wt.%). Among basalts, highest H₂O contents are seen in flank zone eruptions of Surtsey 1963-67 (1.2 ± 0.1 wt.%, 1σ) and Fimmvörðuháls 2010 (0.9 ± 0.1 wt.%) in the SIVZ and in the Berserkjahraun eruption of Ljósufjöll (0.7 ± 0.3 wt.%) in SNVZ. Rift basalts tend to have lower MI H₂O contents, for example 0.36 ± 0.14 wt.% in Holuhraun 2014-15, and 0.23 ± 0.02 wt.% in Fagradalsfjall 2021. The lowest MI H₂O contents are observed in highly trace-element depleted, high-MgO (> 9 wt.%) basalts such as Miðfell (0.07 ± 0.01 wt.%) in the WRZ and Heilagsdalsfjall of Fremrinámar in the NRZ (0.05 ± 0.01 wt.%). Silicic MI H₂O contents from the Askja 1875 eruption vary from 0.6 to 2.7 wt.% (excluding outliers) with an average of 1.6 ± 0.7 %. Compared to Askja, 2-3 times higher average MI H₂O contents are found in the silicic Hekla eruptions 1104 (3.1 ± 1.2 wt.%), H3 (3.5 ± 1.2 wt.%) and H4 (5.7 ± 0.6 wt.%), and the rhyolitic Öræfajökull 1362 (3.1 ± 0.6 wt.%) eruption. Of intermediate Hekla eruptions, the andesitic 1845 and the 1991 basaltic andesite eruptions have MI H₂O contents of $2.1 \pm$ wt.% and 1.2 ± 0.4 wt.%, respectively.

Carbon dioxide: The CO₂ concentrations in Icelandic MIs vary between 0 and 5960 ppm (Fig. 3b), but rarely exceed 3000 ppm. Only basaltic MIs show elevated CO₂ contents, whereas, as a rule, intermediate and silicic MIs have low CO₂ contents (< 50 ppm) that are indistinguishable from matrix glasses. It should be noted that in bubble-bearing melt inclusions, vapor bubbles may host close to 100% of the total MI CO₂ content, but only a few studies have measured and quantified the CO₂ content in the bubbles (Hartley et al., 2014; Neave et al., 2014; Bali et al., 2018). Thus, apparent CO₂ systematics are likely to be affected by sporadic underestimation of true MI CO₂ contents.

Fluorine: Fluorine contents of basaltic MIs range from < 50 ppm in primitive (> 10 wt.% MgO) rift zone basalts to 2850 ppm in the SNVZ Berserkjahraun eruption (Fig. 4c). Apart from Berserkjahraun, all F concentrations in basaltic MIs are below 1000 ppm. Intermediate MIs have between 980-2090 ppm F. Silicic MIs have highly variable F contents from 100 to 2200 ppm. The silicic Askja 1875 MIs lack the high F contents present in the silicic eruptions of Hekla and Öræfajökull with a range of 200-600 ppm. On average, there is no significant

difference between matrix glass and MIs in either average F contents or variability. Fluorine concentrations in plagioclase-hosted MIs are not considered here and are excluded from Figure 3, as they commonly show anomalously high concentrations that reflect the crystallization process rather than the pre-eruptive melt (Neave et al., 2017).

Chlorine: Basaltic MI Cl concentrations vary between 3 and 1900 ppm (Fig. 3d), excluding a single Fimmvörðuháls MI with 2500 ppm. Intermediate MIs (only available from Hekla) have a rather limited Cl range of 210-790 ppm. Silicic MIs have the highest, but most variable Cl contents of 0-2400 ppm.

S2. Effects of crustal magma evolution on H₂O, CO₂, F and Cl

Because of the low solubility of CO₂ at crustal pressures and inferred high CO₂ contents of primary melts, virtually all Icelandic basalts saturate a CO₂-rich vapor phase already at great depth, with only a few possible exceptions (e.g., Hauri et al., 2018; Miller et al., 2019; Matthews et al., 2021; Ranta et al., 2023). As a result, the highest CO₂ contents are typically found in primitive MIs, but are negligible in intermediate and silicic rocks (Fig. 4b). At the other end of the solubility spectrum, H₂O, Cl and F remain undersaturated in basaltic melts at typical Icelandic magma storage pressures, leading to increasing concentrations with decreasing MgO observed in basaltic pillow rim glasses (Nichols et al., 2002; Halldórrsson et al., 2016b) and MIs. For silicic rocks, the H₂O-F-Cl systematics are more complicated. Silicic MIs of single eruptions can have highly variable H₂O-F-Cl contents due to the chained effects of a complicated magmatic history involving fluid exsolution, brine assimilation, recharge, gas fluxing and crustal assimilation that may occur in long-lived (>100 ka) silicic magma mushes in Iceland (Gunnarsson et al., 1998; Schattel et al., 2014; Padilla et al., 2016; Ranta et al., 2021). These effects are smaller at off-rift settings, where silicic magma genesis may approximate closed system fractional crystallization paths (Martin & Sigmarsdóttir, 2007; Schattel et al., 2014), resulting in higher concentrations and smaller variability of H₂O, F and Cl. Opposing behavior is sometimes observed between H₂O and the halogens; for example, silicic Hekla MIs have the highest H₂O concentrations in Iceland, but are the most Cl poor (Fig. 4a, c; Ranta et al., 2021). In summary, the volatile evolution of silicic magmas appears more complicated than that of basalts.

Supplementary Figures

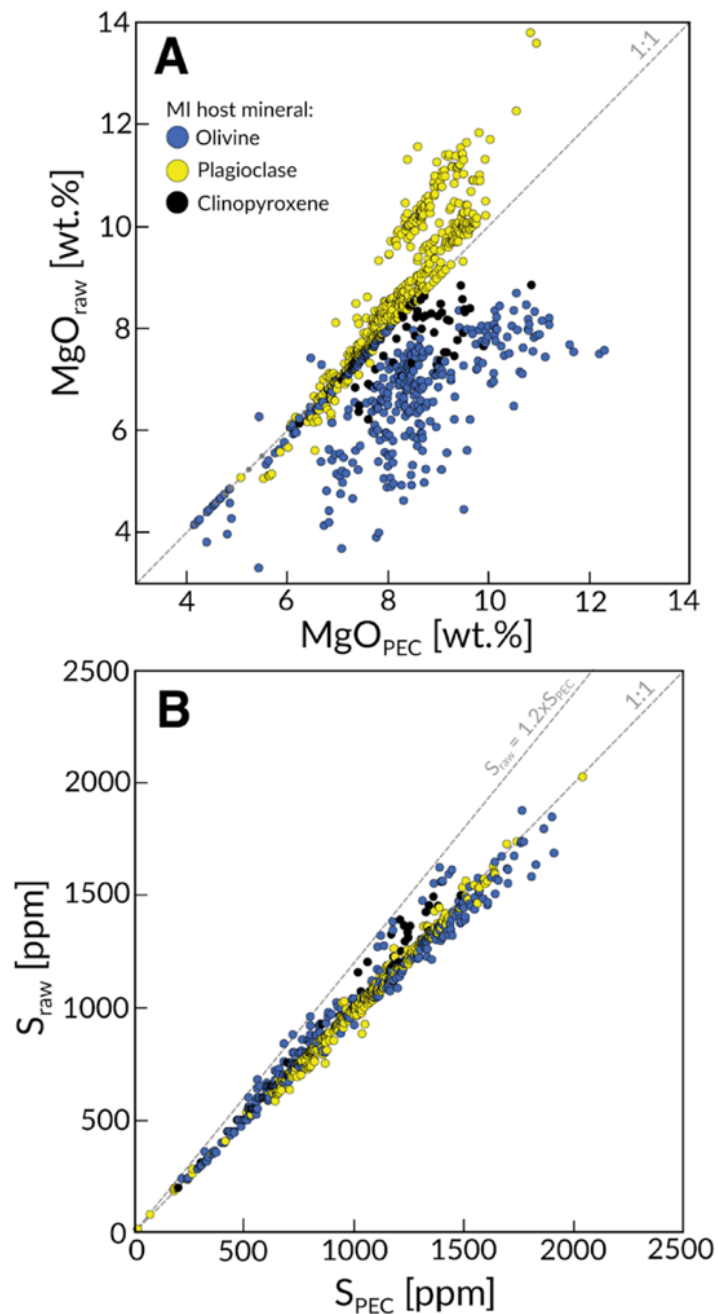


Figure S1. Effects of post-entrainment processes on (a) MgO, and (b) S concentrations of melt inclusions. Subscripts 'raw' and 'PEC' refer to uncorrected raw data and PEP-corrected data, respectively.

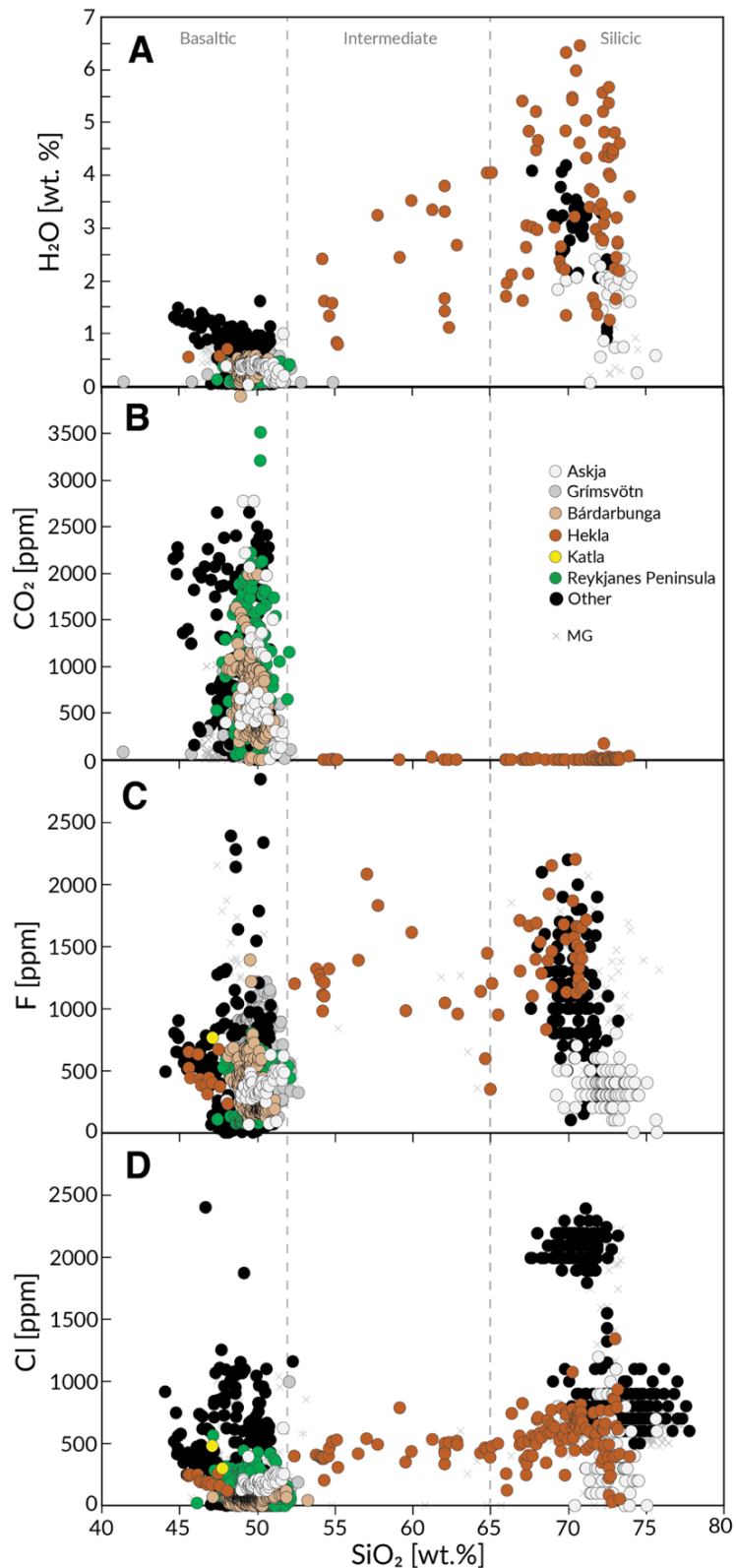


Figure S2. Melt inclusion volatile contents. SiO_2 plotted against (a) H_2O , (b) CO_2 , (c) F and (d) Cl. Data from the Iceland Melt Inclusion Catalogue (IMIC; Table S1)

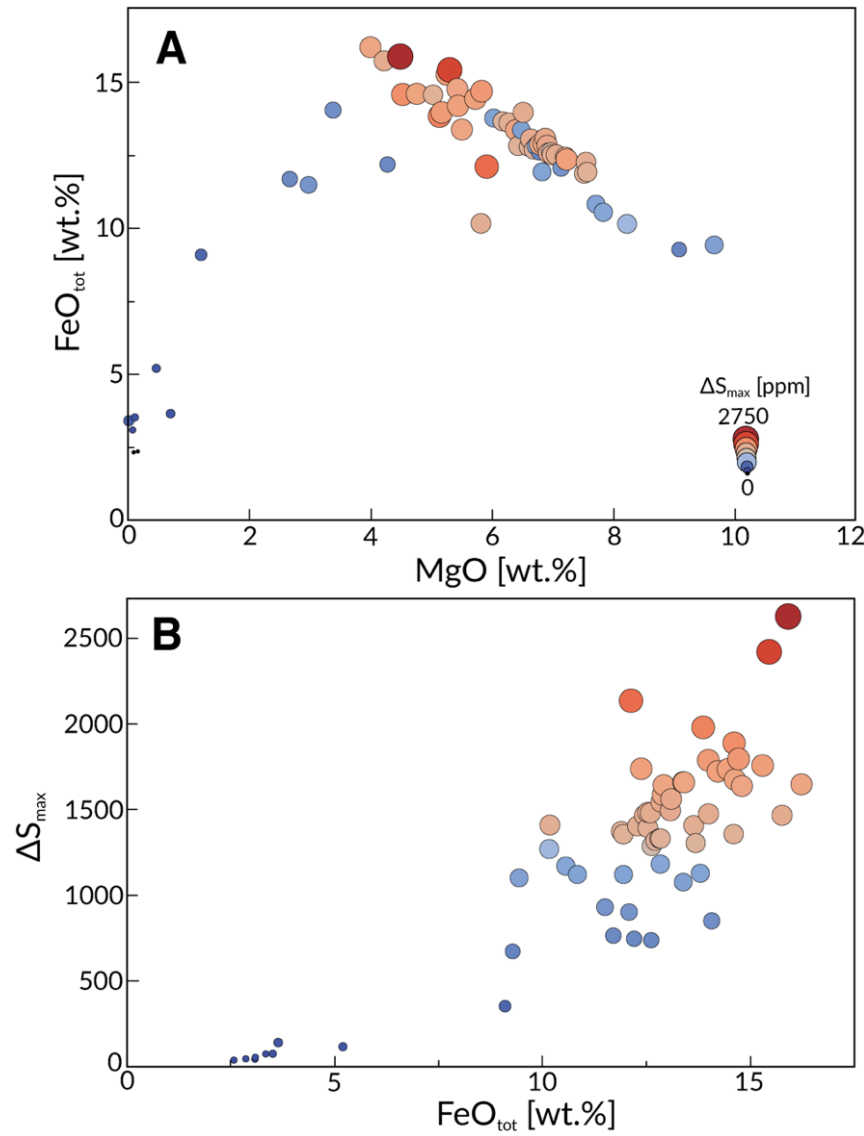


Figure S3. Iron and sulfur. (a) FeO_{tot} vs. MgO. (b) ΔS_{max} vs. FeO_{tot}. FeO content of melts is one of the main controls on sulfur solubility (Smythe et al., 2017), resulting in a broad correlation between ΔS_{max} and FeO_{tot}. However, large variability (> 100%) in ΔS_{max} is observed at a given FeO_{tot}, demonstrating the juxtaposed effects of pressure, temperature and $f\text{O}_2$ on the SCSS, as well as the likely presence of sulfide-undersaturated melts at higher MgO. Circles represent individual eruptions and are shaded from blue to red and increase in size with increasing ΔS_{max}.

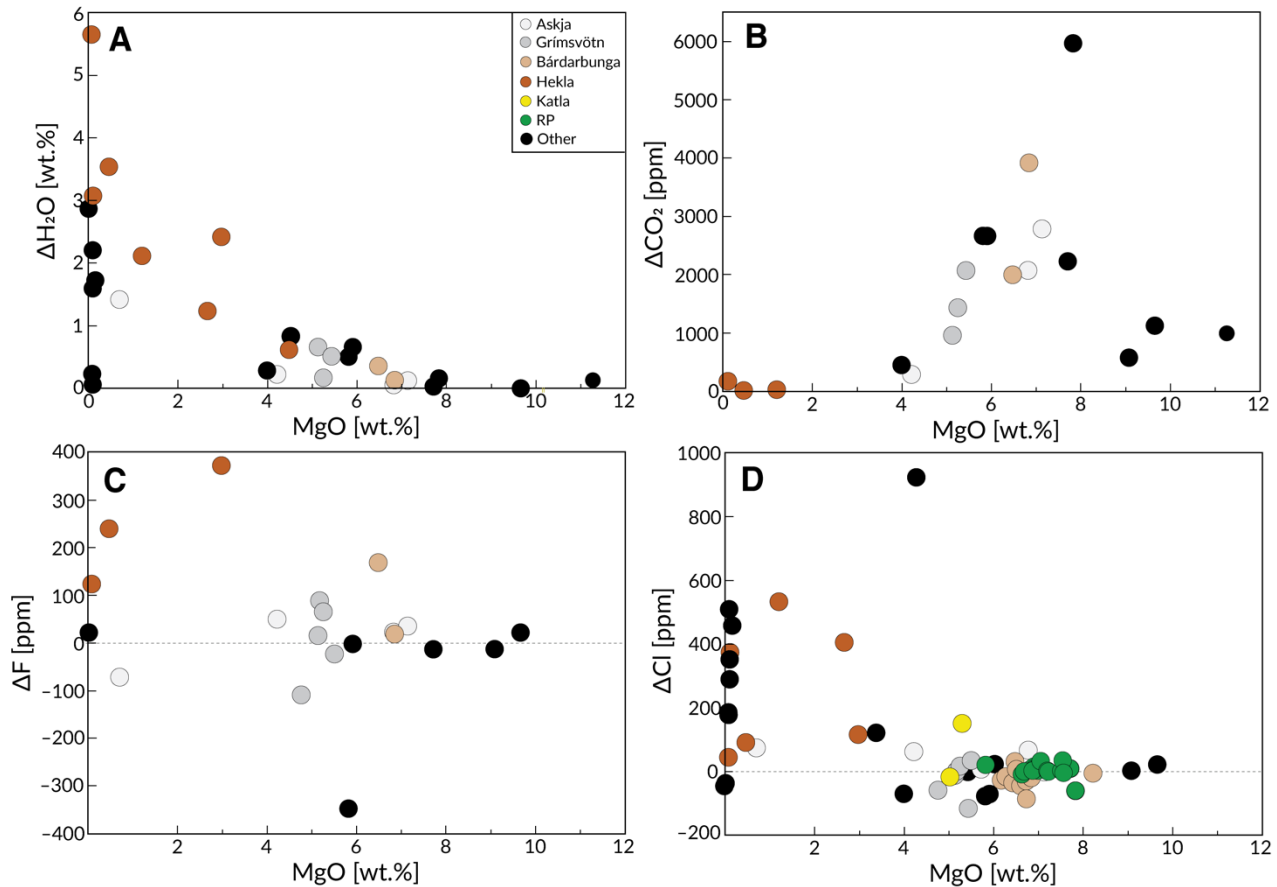


Figure S4. Application of the petrological method for (a) H_2O , (b) CO_2 , (c) Cl and (d) F vs. MgO . The volatile emission estimates for these volatiles are not considered to be as accurate as for sulfur (see Section 5)

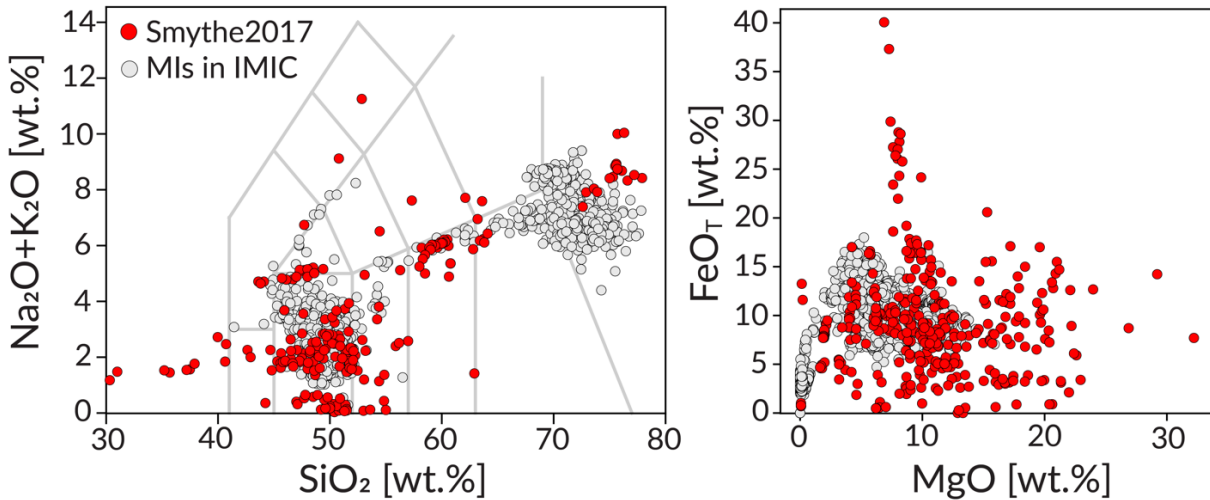


Figure S5. Calibration range of the Smythe et al. (2017) $\text{S}^2\text{-CSS}$ model compared to IMIC MI data. The two mostly overlap, suggesting that the Smythe et al. (2017) is an appropriate model for Icelandic MIs.

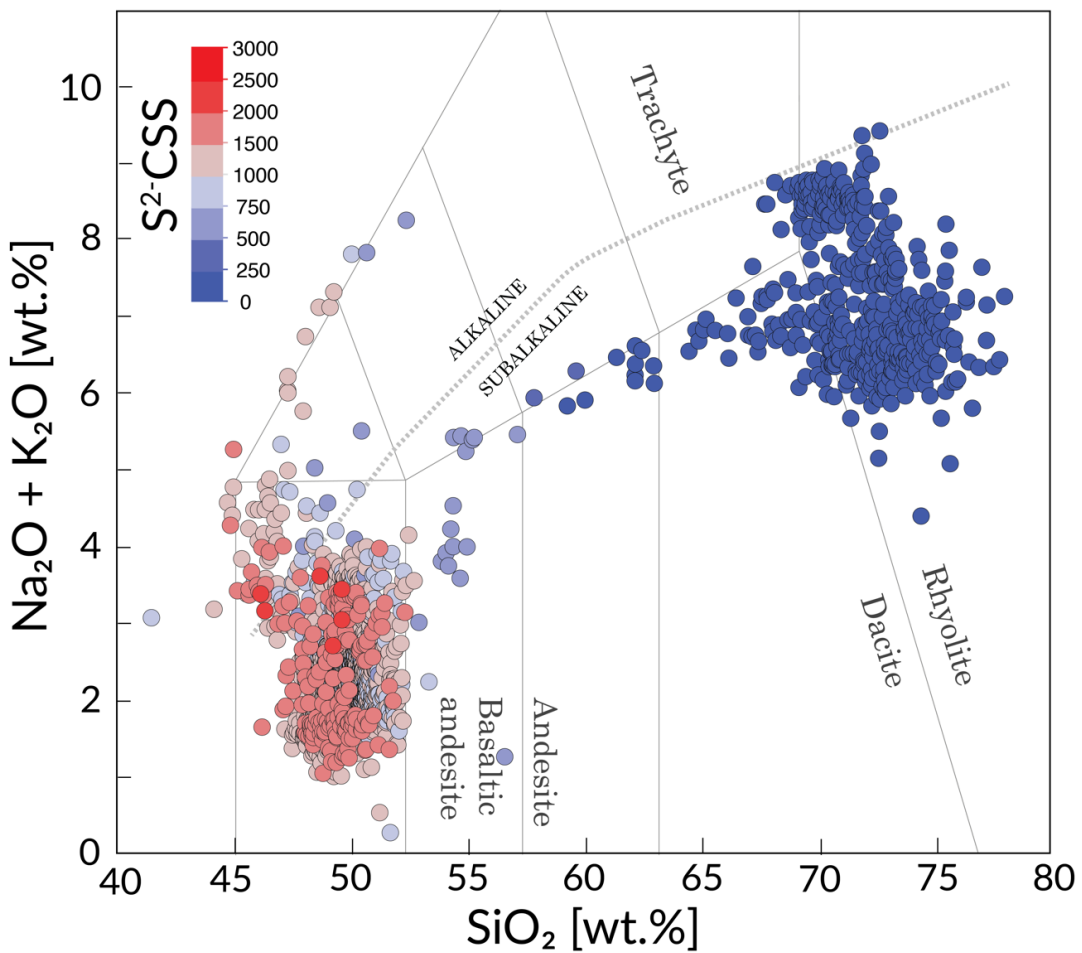


Figure S6. Total alkali versus silica (TAS) diagram. IMIC MI data are plotted and colored after their $\text{S}^2\text{-CSS}$ calculated after Smythe et al. (2017) implemented in PySulfSat (Wieser & Gleeson, 2023). The figure illustrates that variations in the alkalinity of Icelandic melts does not, in a major way, affect $\text{S}^2\text{-CSS}$. See Table S8 for model parameters.

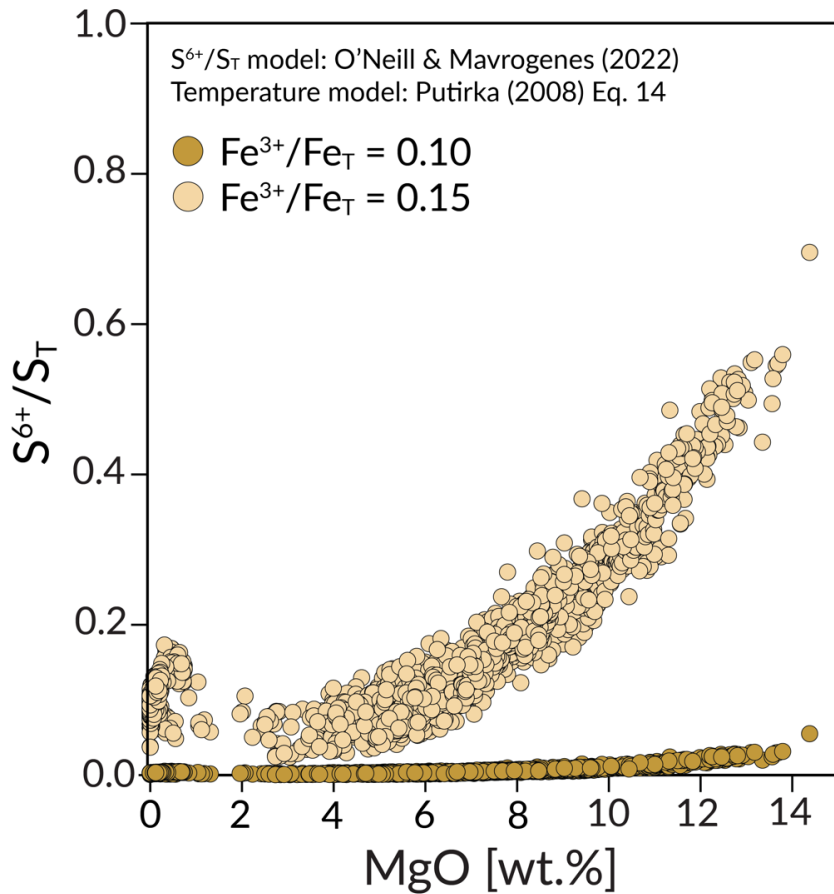


Figure S7. Effect of varying melt Fe^{3+}/Fe_T on melt S^{6+}/S_T . The S^{6+}/S_T was calculated for each raw MI composition in IMIC using the model of O'Neill & Mavrogenes (2022) implemented in PySulfSat (Wieser & Gleeson, 2022). Melt temperatures, used for the S^{6+}/S_T calculation, were calculated with Eq.14 of Putirka (2008). The Fe^{3+}/Fe_T range represents the variability found in subglacial glasses in Iceland measured by Mössbauer spectroscopy (Óskarsson et al., 1994)

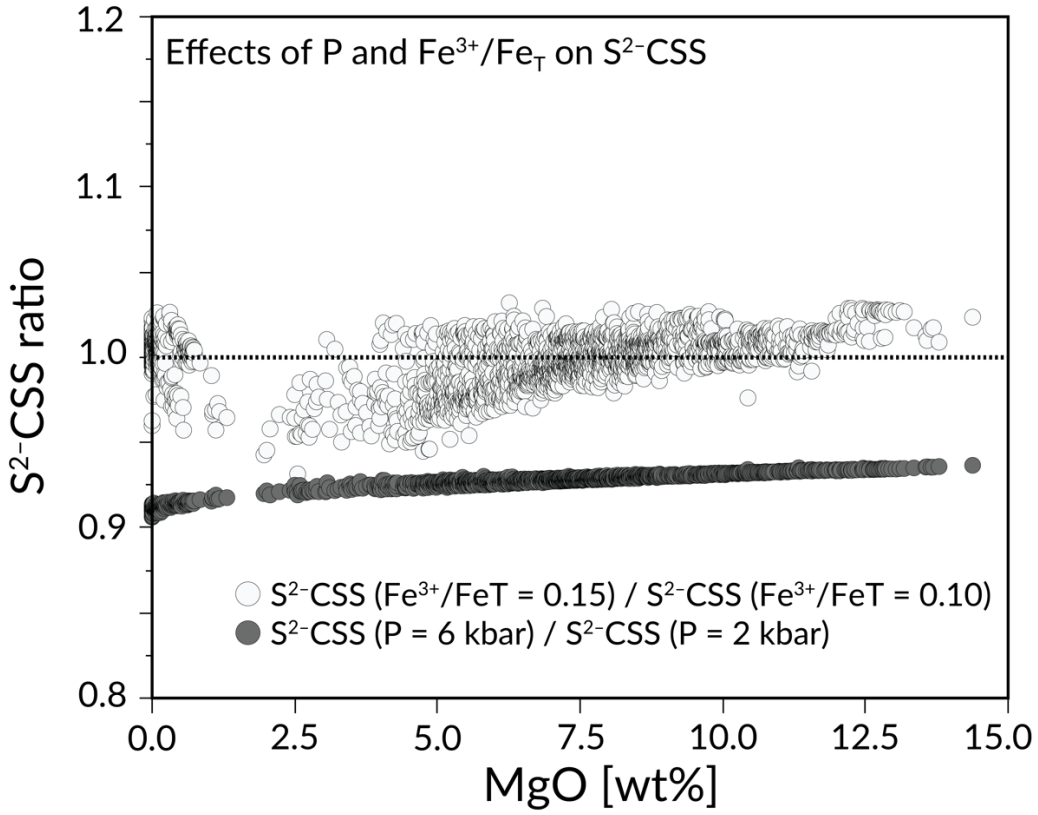


Figure S8. The effect of pressure (P) and $\text{Fe}^{3+}/\text{Fe}_T$ on $\text{S}^2\text{-CSS}$. The $\text{S}^2\text{-CSS}$ was calculated for IMIC raw MI data after Smythe et al. (2017), for two example cases with varying pressure (2 and 6 kbar, dark grey) and $\text{Fe}^{3+}/\text{Fe}_T$ (0.10 and 0.15, light grey). The curves illustrate the small effect of $\text{Fe}^{3+}/\text{Fe}_T$ on the $\text{S}^2\text{-CSS}$ (although its effect on S^{6+}/Sr and thereby dissolved S^{6+} and STCSS is considerable, see Figs. 7 and S7) and the negative effect of increasing P. Models were implemented in PySulfSat (Wieser & Gleeson, 2022). Remaining model parameters are same as in Fig. 7 and Table S8.

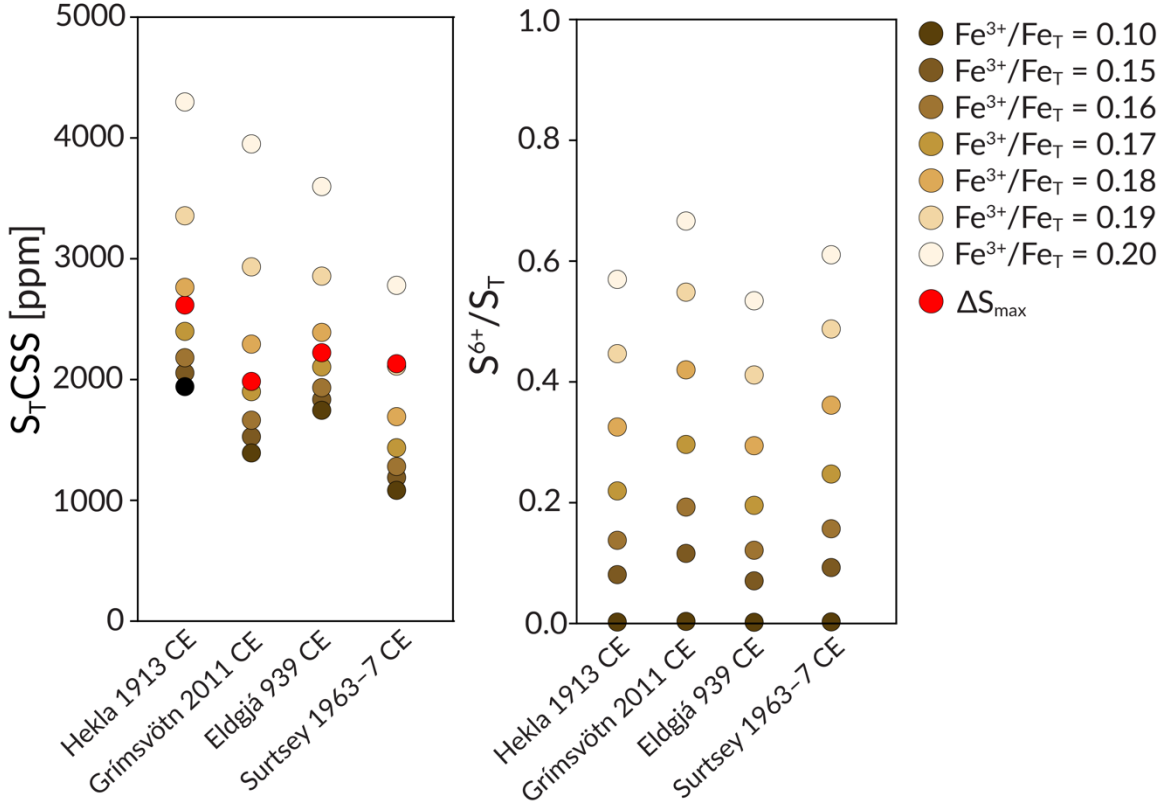


Figure S9. Effect of $\text{Fe}^{3+}/\text{Fe}_{\text{T}}$ on $S_{\text{t}}\text{CSS}$ and S^{6+}/S_{t} for the four Icelandic eruptions with highest S emission potentials (Table 2). The S^{6+}/S_{t} was calculated for average matrix glass compositions (Table S2) of each eruption in IMIC using the model of O'Neill & Mavrogenes (2022) implemented in PySulfSat (Wieser & Gleeson, 2022). Melt temperatures were calculated with Eq.14 of Putirka (2008). For the melt $S_{\text{t}}\text{CSS}$ to match maximum eruptible S contents (red circles), $\text{Fe}^{3+}/\text{Fe}_{\text{T}}$ of between 0.17 and 0.18 are required for Hekla 1913 CE, Grímsvötn 2011 CE and Eldgjá 939 CE eruptions, and about 0.19 for the Surtsey 1963–7 CE eruption. Notably, the maximum $\text{Fe}^{3+}/\text{Fe}_{\text{T}}$ value measured in Surtsey tephra glass is considerably lower at 0.155 (Schipper & Moussallam, 2017). Spinel–olivine oxybarometry suggests relatively oxidized magmatic conditions ($\Delta\text{FMQ} \approx 0.1\text{--}0.5$) for two 500–700 ka ankaramites erupted at the Eyjafjallajökull volcano in the SIVZ (Nikkola et al., 2017).

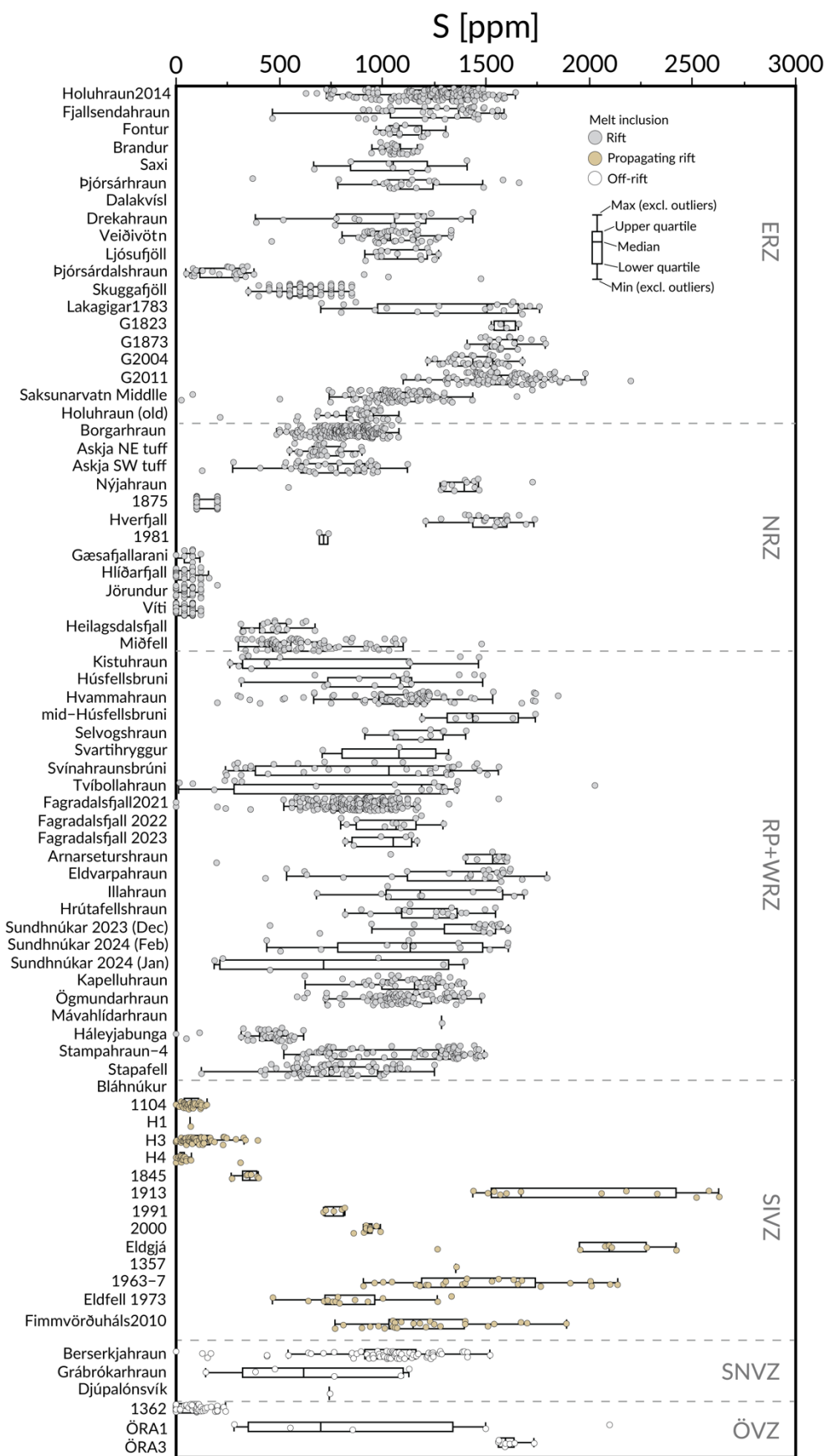
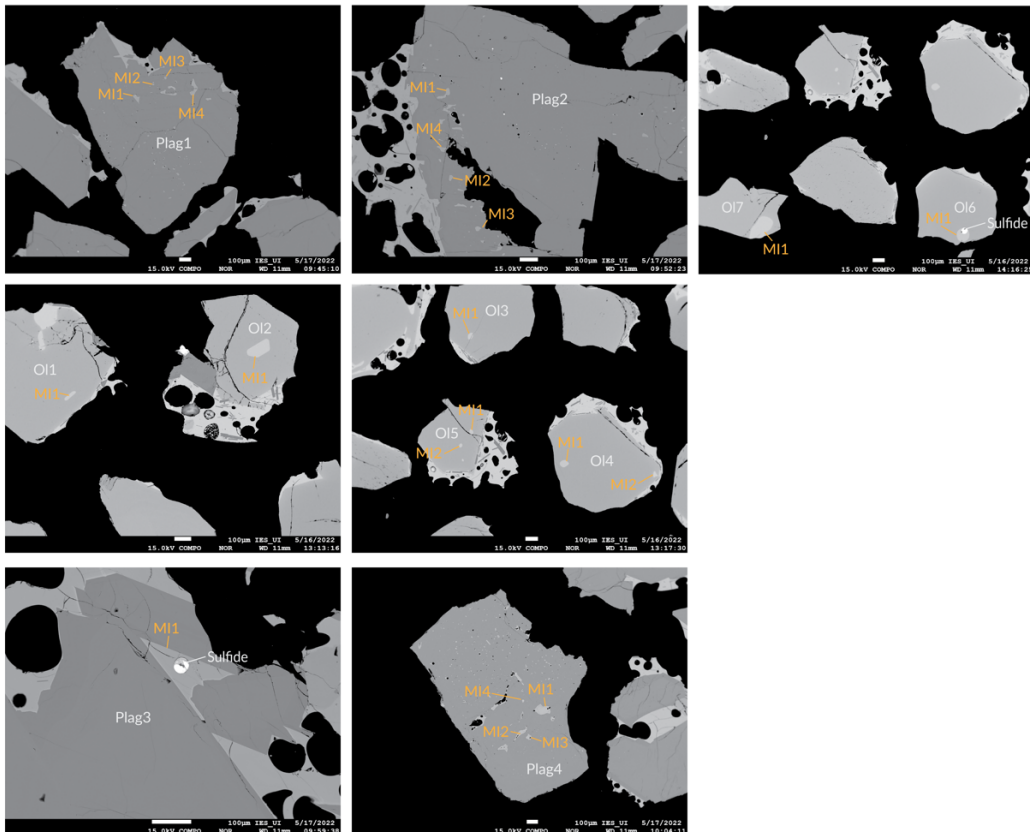


Figure S10 (above). Box-and-whiskers plot of melt inclusion S contents divided by eruption. Data are arranged by tectonic setting and volcanic zone.

FJ5a



FJ6a

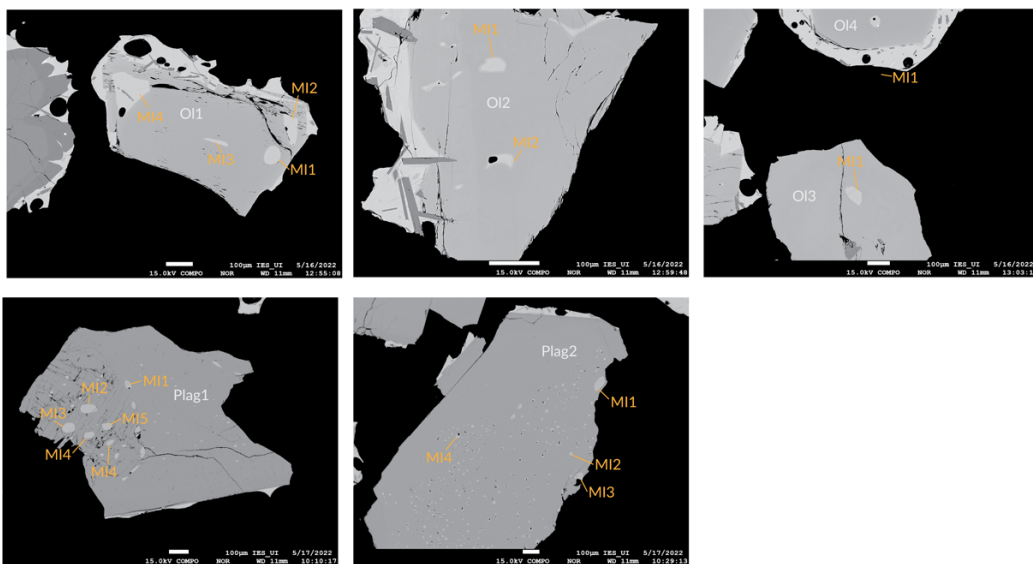
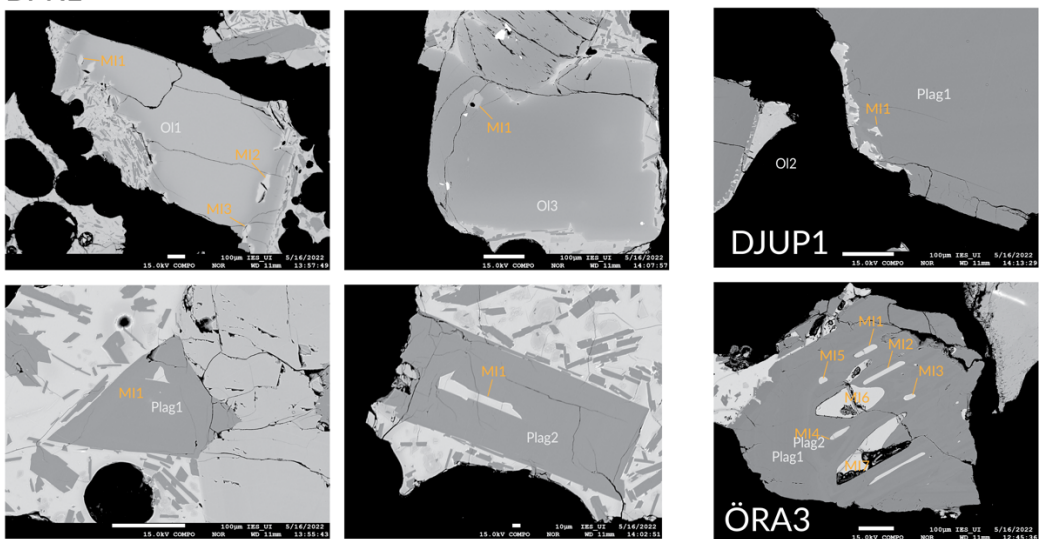
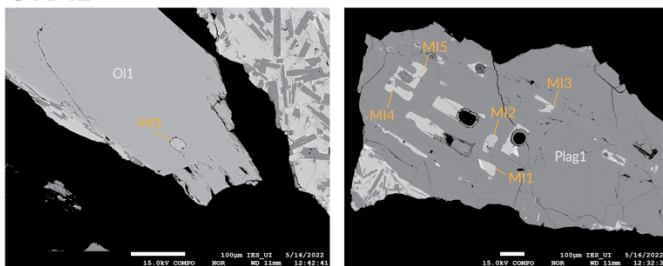


Fig. S11. Backscattered-electron images of melt inclusions and their host crystals analyzed in this study (continuous on next page).

BFR1



ÖRA1



ELD2



ELD1

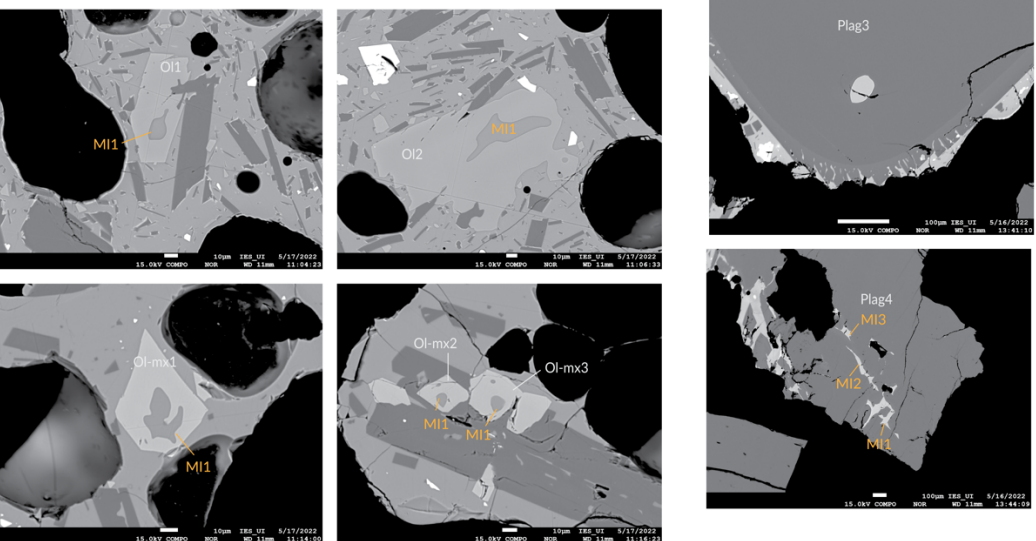


Fig. S11. (cont.)